The Second-Order Condition for the Dielectric Interface Orthogonal to the Yee-Lattice Axis in the FDTD Scheme

T. Hirono, *Member, IEEE*, Y. Shibata, W. W. Lui, *Member, IEEE*, S. Seki, *Senior Member, IEEE*, and Y. Yoshikuni, *Member, IEEE*

***Abstract*—The reflection coefficient at the dielectric interface orthogonal to the Yee-lattice axis in the finite-difference time-domain scheme is explicitly obtained. In the expression, the effective permittivities assigned to the nodes in the vicinity of the interface are included as parameters. The suitable effective permittivities for the accurate modeling of the interface are investigated theoretically based on the reflection coefficient. Regardless of the angular frequency, the incident angle, and the interface position relative to the lattice, second-order accuracy is achieved by the use of effective permittivies based on the weighted harmonic mean and arithmetic mean of the material permittivities. The second-order accuracy is demonstrated by numerical examples.**

***Index Terms*—Electromagnetic fields, FDTD methods, numerical analysis, time domain analysis.**

I. Introduction

THE finite-difference time-domain (FDTD) scheme has been used extensively for electromagnetic field simulation [1], [2]. In such a simulation, accurate modeling of the material interface is an important issue. The standard FDTD scheme for the homogeneous media is second-order accurate in space. The accuracy may be degraded in applications to inhomogeneous media. For the dielectric-PEC (perfect electric conductor) interface, several methods, including a staircase approximation [3], [4], and a local reformulation of the scheme [5], [6], have been proposed. The error of the methods has been assessed theoretically in [3], [7], in which the data concerning the order of accuracy were presented. For the dielectric-dielectric interface, the use of the effective permittivities assigned to the nodes near the interface has been proposed [8], [9]. However, the performance has not been analyzed theoretically.

In this letter, the reflection coefficient of the dielectric–dielectric interface orthogonal to the Yee-lattice axis is derived explicitly considering the effective permittivities in the vicinity of the interface. Based on the reflection coefficient, effective permittivities suitable for second-order accuracy are obtained.

Manuscript received April 6, 2000; revised June 20, 2000.

T. Hirono, Y. Shibata, S. Seki, and Y. Yoshikuni are with NTT Photonics Laboratories, Atsugi-shi, Kanagawa, 243-0198, Japan (e-mail: tuhirono@aecl.ntt.co.jp).

W. W. Lui is with Lightwave Microsystems, San Jose, CA 95134 USA.

Publisher Item Identifier S 1051-8207(00)08452-X.

II. Formulation

First, we explain the situation in which the incident plane wave does not have a magnetic component orthogonal to the interface. The starting point is the two-dimensional (2-D) TE$_y$ polarization case, and the analyzed $x-z$ plane is shown in Fig. 1. The cell widths are Δ_x and Δ_z. The time increment is Δ_t. The material permittivity is ε_1 for region $z < d\Delta_z$ and ε_2 for region $z > d\Delta_z$, where d is the offset ratio ($0 \leqq d \leqq 1/2$). We assume that, in the simulation, the effective permittivities ε_{ot} and ε_{pl} are, respectively, assigned to the E_z and E_x nodes nearest the interface. The incident, transmitted, and reflected waves are time-harmonic plane waves with numerical angular frequency ω. All wavevector components in the x direction are equal and expressed as k_x. The H_y components of the incident and reflected waves are, respectively, expressed as $H_{y,1}\exp(j(-k_x x - k_{z,1}z + \omega t))$ and $H_{y,3}\exp(j(-k_x x - k_{z,3}z + \omega t))$ in region $z \leqq -\Delta_z/2$. The component $k_{z,1}$ is positive and $k_{z,3} = -k_{z,1}$. The H_y component of the transmitted wave is expressed as $H_{y,2}\exp(j(-k_x x - k_{z,2}z + \omega t))$ in region $z \geqq \Delta_z/2$. The incident and transmitted angles are, respectively, defined as $\theta_1 = \tan^{-1}(k_x/k_{z,1})$ and $\theta_2 = \tan^{-1}(k_x/k_{z,2})$. When the expressions for the electric and magnetic components of the waves are substituted into the FDTD equations for the time-evolution of the E_x component on the ε_{pl} node, the E_z component on the ε_{ot} node, and the H_y component on the node between the ε_{ot} nodes, three equations including $H_{y,1}$, $H_{y,2}$, and $H_{y,3}$ are obtained. By solving the equations, the reflection coefficient $R(=H_{y,3}/H_{y,1})$ is explicitly expressed as

$$R = \frac{P}{Q}, \tag{1}$$

$$\begin{aligned} P = {} & \frac{\cos\Theta_1}{\sqrt{\varepsilon_1}} - \frac{\cos\Theta_2 e^{j\Delta_z((k_{z,1}-k_{z,2})/2)}}{\sqrt{\varepsilon_2}} \\ & - (\Delta_z)^2\mu\varepsilon_{pl}W^2\left(1 - \frac{K_{pl}^2}{\varepsilon_{ot}\mu W^2}\right)\frac{\cos\Theta_1}{\sqrt{\varepsilon_1}} \\ & + j\Delta_z\sqrt{\mu}W\left\{-\left(1 - \frac{K_{pl}^2}{\varepsilon_{ot}\mu W^2}\right)e^{j\Delta_z(k_{z,1}/2)} \right. \\ & \left. + \frac{\varepsilon_{pl}\cos\Theta_1\cos\Theta_2 e^{-(j\Delta_z k_{z,2}/2)}}{\sqrt{\varepsilon_1\varepsilon_2}}\right\} \end{aligned} \tag{2}$$

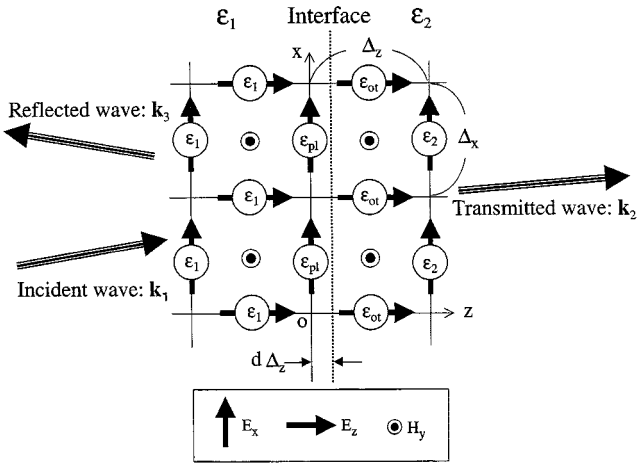

Fig. 1. Schematic drawing of the analyzed $x-z$ plane for the reflection coefficient calculation in the 2-D TE$_y$ polarization case.

$$Q=\frac{\cos\Theta_1}{\sqrt{\varepsilon_1}}+\frac{\cos\Theta_2 e^{-j\,\Delta_z(k_{z,1}+k_{z,2})/2}}{\sqrt{\varepsilon_2}} -(\Delta_z)^2\mu\varepsilon_{pl}W^2\left(1-\frac{K_{pl}^2}{\varepsilon_{ot}\mu W^2}\right)\frac{\cos\Theta_1}{\sqrt{\varepsilon_1}} +j\,\Delta_z\sqrt{\mu}W\left\{\left(1-\frac{K_{pl}^2}{\varepsilon_{ot}\mu W^2}\right)e^{-j\,\Delta_z(k_{z,1}/2)} +\frac{\varepsilon_{pl}\cos\Theta_1\cos\Theta_2 e^{-(j\,\Delta_z k_{z,2}/2)}}{\sqrt{\varepsilon_1\varepsilon_2}}\right\} \tag{3}$$

$$W=2\sin(\omega\,\Delta_t/2)/\Delta_t,\quad K_{pl}^2=K_x^2$$
$$K_x=2\sin(k_x\Delta_x/2)/\Delta_x \tag{4}$$
$$\Theta_i=\tan^{-1}(K_x/K_{z,i}),\qquad (i=1,\quad 2) \tag{5}$$
$$K_{z,i}=2\sin(k_{z,i}\,\Delta_z/2)/\Delta_z,\qquad (i=1,\quad 2) \tag{6}$$

where μ is the permeability. For the accuracy assessment, the product of R and $\exp(2jk_{z,1}\,d\,\Delta_z)$, which account for the phase shift owing to the change of interface position, is compared to the Fresnel's reflection coefficient [10]. If the product is expanded in the power series of Δ_z as

$$e^{2j\,k_{z,1}\,d\,\Delta_z}R=\frac{e^{j(k_{z,1}+k_{z,2})\,d\,\Delta_z}P}{e^{j(-k_{z,1}+k_{z,2})\,d\,\Delta_z}Q} =\frac{\dfrac{\cos\theta_1}{\sqrt{\varepsilon_1}}-\dfrac{\cos\theta_2}{\sqrt{\varepsilon_2}}+A\,\Delta_z+O(\Delta_z^2)}{\dfrac{\cos\theta_1}{\sqrt{\varepsilon_1}}+\dfrac{\cos\theta_2}{\sqrt{\varepsilon_2}}+B\,\Delta_z+O(\Delta_z^2)} \tag{7}$$

the coefficients of the first-order terms, A and B, are expressed as

$$A=-j\mu\omega(-C+D),\quad B=-j\,\mu\omega(C+D) \tag{8}$$
$$C=\cos^2\theta_1\,d+\cos^2\theta_2(1-d)-\left(1-\frac{\varepsilon_1\sin^2\theta_1}{\varepsilon_{ot}}\right) \tag{9}$$
$$D=\left\{\sqrt{\frac{\varepsilon_2}{\varepsilon_1}}\left(\frac{1}{2}-d\right)+\sqrt{\frac{\varepsilon_1}{\varepsilon_2}}\left(\frac{1}{2}+d\right)-\frac{\varepsilon_{pl}}{\sqrt{\varepsilon_2\varepsilon_1}}\right\} \cdot\cos\theta_1\cos\theta_2. \tag{10}$$

If ε_{ot} and ε_{pl} are given by

$$\frac{1}{\varepsilon_{ot}}=\frac{d}{\varepsilon_1}+\frac{1-d}{\varepsilon_2} \tag{11}$$
$$\varepsilon_{pl}=\left(\tfrac{1}{2}+d\right)\varepsilon_1+\left(\tfrac{1}{2}-d\right)\varepsilon_2 \tag{12}$$

terms C and D vanish. Here, the following FDTD version of "Snell's law" is used in the manipulation of (9):

$$\sqrt{\varepsilon_1}\sin\theta_1=\sqrt{\varepsilon_2}\sin\theta_2+O(\Delta_z^2). \tag{13}$$

When ε_{ot} and ε_{pl} as expressed by (11) and (12) are used, R approximates the exact reflection coefficient at the second-order in Δ_z for any angular frequency ω, any incident angle θ_1, and any offset ratio d in the range $0\leqq d\leqq 1/2$. The explicit expression for the reflection coefficient, R, is also obtained for the offset ratio out of that range. The suitable effective permittivities are examined based on the expression. In general, the effective permittivity for the second-order accuracy is the weighted arithmetic mean of the material permittivities in the surrounding cell for the E_x node and the weighted harmonic mean for the E_z node. The accuracy increment by the effective permittivity based on the weighted harmonic mean has been proposed [9]. Here, we have theoretically proved its second-order accuracy for the first time.

The above calculations are extended straightforwardly to the three-dimensional situation with the Yee lattice, whose section at the $x-z$ plane is shown in Fig. 1. The interface is the plane expressed as $z=d\Delta_z(0\leqq d\leqq 1/2)$. The components, H_x, H_y, E_x, E_y, and E_z are considered. In this situation, all wavevector components in the y direction are also equal and expressed as k_y. When the definitions of K_{pl}^2, Θ_1, and Θ_2 are modified as

$$K_{pl}^2=K_x^2+K_y^2,\quad K_y=2\sin(k_y\,\Delta_y/2)/\Delta_y, \tag{14}$$
$$\Theta_i=\tan^{-1}\left(\sqrt{K_x^2+K_y^2}/K_{z,i}\right)\qquad (i=1,\,2) \tag{15}$$

the reflection coefficient for the magnetic components is also expressed by (1)–(3). The effective permittivities for the second-order accuracy are again expressed by (11) and (12).

For the incident plane wave without the electric-component orthogonal to the interface, the reflection coefficient is calculated similarly. The second-order accuracy is achieved when the effective permittivity equal to the weighted arithmetic mean of the material permittivities in the surrounding cell is assigned to the electric-component nodes in the vicinity of the interface.

III. Numerical Examples

Here, two numerical examples in the 2-D TE$_y$ polarization case are presented. First, the wave-propagation along the waveguide was simulated. The waveguide structure is illustrated in Fig. 2. The offset ratio of one core-cladding interface was set to 0 and the offset ratio of the other interface was changed

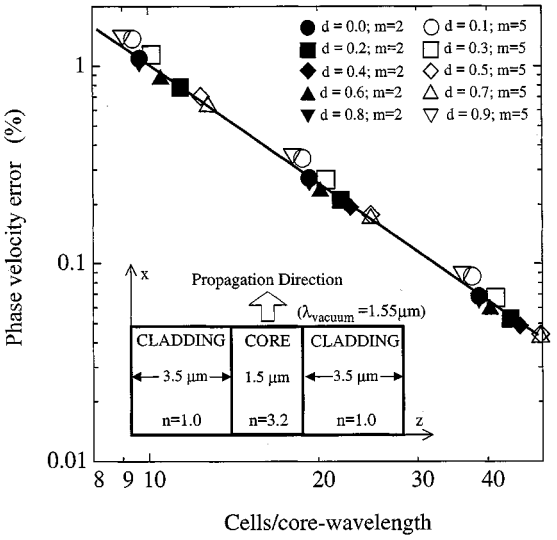

Fig. 2. Phase velocity errors in the simulations of wave propagation in the second- and fifth-mode of the waveguide. The waveguide supports six modes. The incident angles are 61.4° for the second mode and 22.1° for the fifth mode. d is the offset ratio at the core-cladding interface and m is the mode number. In the inset, n is the refractive index.

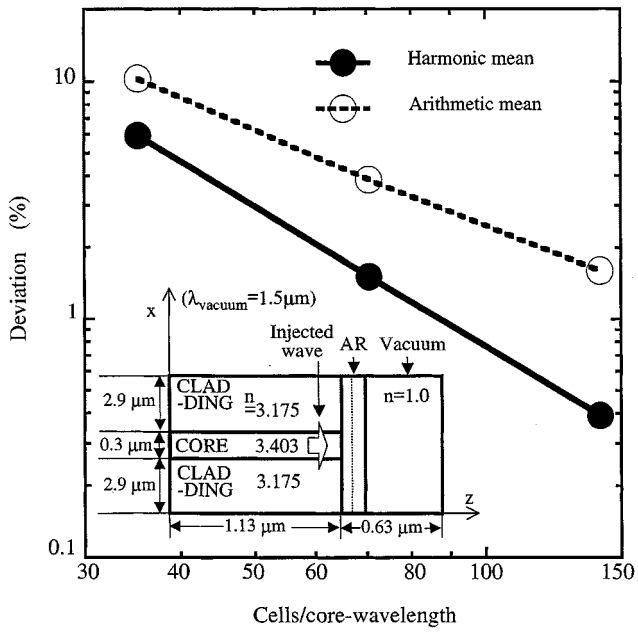

Fig. 3. Deviations in the simulated power reflectivity at the coated facet from its extrapolated value. In the inset, n is the refractive index and AR represents the dielectric coatings. The refractive index and the thickness are 2.257 and 0.125 μm for the first coating and 1.455 and 0.175 μm for the second coating.

in each simulation. The effective permittivities for the second order accuracy were assigned to the E_z and E_x nodes in the vicinity of the latter interface. The Courant–Friedrichs–Lewy (CFL) number was 0.577. Fig. 2 shows the phase velocity errors for the second and fifth modes as a function of the cell-number per wavelength in the core. Second order accuracy is obtained for both modes and all offset ratios.

Next, the waveguide-facet reflection was simulated. The waveguide was truncated and the facet was coated with two dielectric layers for anti-reflection. The whole simulated domain was surrounded by a 16-cell PML absorber [11], [12]. The domain is illustrated in Fig. 3. The cells were square and Δ_x was 0.0125, 0.006 25, or 0.003 125 μm in each simulation. All material interfaces were located on nodes of the electric components whose directions were orthogonal to the interfaces. Two cases of effective permittivity assignment for the nodes at the interfaces were tested. One case was the harmonic mean of the permittivities on both sides. The other was the arithmetic mean. The analysis in the previous section shows that the former case gives second-order accuracy and the latter first-order accuracy. The wave in the 0th mode was injected toward the facet and the reflected power was evaluated by the single-precision numerical calculation. The CFL number was 0.7. The extrapolated power reflectivity toward $\Delta_z = 0$ was 0.015 448% for the former case and 0.015 457% for the latter. Fig. 3 shows the reflectivity deviations from the extrapolated values as a function of the cell-number per wavelength in the core. Second-order accuracy in the use of the harmonic mean is clearly obtained. The slope of the curve for the arithmetic mean approaches that corresponding to the first-order accuracy as the cell number increases.

REFERENCES

[1] K. S. Yee, "Numerical solution of initial boundary value problems involving Maxwell's equations in isotropic media," *IEEE Trans. Antennas Propagat.*, vol. AP-14, pp. 302–307, May 1966.

[2] A. Taflove, *Computational Electrodynamics, the Finite-Difference Time-Domain Method*. Norwood, MA: Artech House, 1995.

[3] A. C. Cangellaris and D. B. Wright, "Analysis of the numerical error caused by the stair-stepped approximation of a conducting boundary in FDTD simulations of electromagnetic phenomena," *IEEE Trans. Antennas Propagat.*, vol. 39, pp. 1518–1525, Oct. 1991.

[4] J. B. Schneider and K. L. Schlager, "FDTD simulations of TEM horns and the implications for staircased representations," *IEEE Trans. Antennas Propagat.*, vol. 45, pp. 1830–1838, Dec. 1997.

[5] T. M. Jurgens, A. Taflove, K. Umashankar, and T. G. Moore, "Finite-difference time-domain modeling of curved surfaces," *IEEE Trans. Antennas Propagat.*, vol. 40, pp. 357–366, Apr. 1992.

[6] S. Dey and R. Mittra, "A locally conformal finite-difference time-domain (FDTD) algorithm for modeling three-dimensional perfectly conducting objects," *IEEE Microwave Guided Wave Lett.*, vol. 7, pp. 273–275, Sept. 1997.

[7] C. J. Railton and J. B. Schneider, "An analytical and numerical analysis of several locally conformal FDTD schemes," *IEEE Trans. Microwave Theory Tech.*, vol. 47, pp. 56–66, Jan. 1999.

[8] X. Zhang and K. K. Mei, "Time-domain finite difference approach to the calculation of the frequency-dependent characteristics of microstrip discontinuities," *IEEE Trans. Microwave Theory Tech.*, vol. 36, pp. 1775–1787, Dec. 1988.

[9] M. Celuch-Marcysiak and W. K. Gwarek, "Higher-order modeling of media interfaces for enhanced FDTD analysis of microwave circuits," in *Proc. 24th European Microwave Conf.*, Cannes, France, 1994, pp. 1530–1535.

[10] M. Born and E. Wolf, *Principles of Optics*. Oxford, U.K.: Pergamon, 1980, p. 40.

[11] J.-P. Berenger, "A perfectly matched layer for the absorption of electromagnetic waves," *J. Comput. Phys.*, vol. 114, pp. 185–200, Oct. 1994.

[12] J. Yamauchi, M. Mita, S. Aoki, and H. Nakano, "Analysis of antireflection coatings using the FD–TD method with the PML absorbing boundary condition," *IEEE Photon. Technol. Lett.*, vol. 8, pp. 239–241, Feb. 1996.